

¹
² Delayed introduction and susceptible variation drive spatial
³ asynchrony in pertussis epidemics

⁴
⁵ Sang Woo Park^{1,*}

⁶ **1** School of Biological Sciences, Seoul National University, Seoul, Korea

⁷ *Corresponding author: sangwoopark@snu.ac.kr

⁸ **Abstract**

⁹ Infectious disease outbreaks typically exhibit a large-scale, spatial synchrony, re-
¹⁰ flecting coupling through shared environmental forcing and human mobility. Dur-
¹¹ ing South Korea's unprecedented large pertussis outbreak in 2024—2025, however,
¹² asynchronous epidemic patterns were observed throughout the country: some regions
¹³ experienced two epidemic waves, while others regions experienced only the first or
¹⁴ second wave. Using high-resolution surveillance data from 252 municipalities and a
¹⁵ simple transmission model, we show that heterogeneity in introduction timing and
¹⁶ local susceptibility can drive such fine-scale asynchrony even when transmission is
¹⁷ spatially homogeneous. These results redefine epidemic synchrony as a condition
¹⁸ contingent not only on shared transmission dynamics, but also on variation in initial
¹⁹ epidemic conditions.

20 **Introduction**

21 Spatiotemporal variation in epidemic dynamics offers a powerful means for under-
22 standing factors that determine the timing and magnitude of epidemic waves across
23 populations [1, 2, 3, 4]. Ecological theory predicts that spatial coupling—via shared
24 environmental forcing and human mobility—can synchronize epidemic dynamics be-
25 tween neighboring locations, sometimes manifesting as travelling waves, where epi-
26 demic waves propagate through space [5, 6, 7]. Consistent with this theory, large-
27 scale spatial synchrony has been observed across diverse pathogens, including measles
28 [7], dengue [8], influenza [9], RSV [4], and SARS-CoV-2 [10], highlighting the ubiq-
29 uituity of spatial coupling in shaping epidemic dynamics.

30 Between 2024 and 2025, an unprecedented large pertussis outbreak occurred in
31 Korea, resulting in more than 50,000 cases by early 2025 (Figure 1) [11]. This out-
32 break marked a dramatic increase in the disease compared to 292 cases reported in
33 2023 and 21 cases reported in 2022, despite high vaccine coverage (91.1% of identified
34 2024 cases had a known vaccination history) [12, 11]. The outbreak consisted of two
35 waves that peaked around late July and December 2024 (Figure 1A) and exhibited
36 large spatial heterogeneity in timing (Figure 1B,C) and magnitude (Figure 1D). For
37 example, both Seoul, the capital city located in the northwest region, and Busan,
38 the second most populated city located at the southeast end, experienced two waves,
39 whereas Daegu, the fourth most populated city located < 100km away from Busan,
40 only experienced the second wave (Figure 1C; see Figure S1 for epidemic dynam-
41 ics in other regions). This pronounced asynchrony deviates from our expectations
42 based on spatial coupling, raising questions about mechanisms driving this fine-scale
43 spatiotemporal heterogeneity in pertussis epidemic [13].

44 To address this question, we combine a detailed spatiotemporal surveillance data
45 from 252 municipalities in Korea (Figure 1) with mathematical modeling approaches.
46 We begin by showing that asynchrony in pertussis epidemics, captured by heteroge-
47 neous epidemic timing, is associated with differences in introduction delays. In con-
48 trast, the analysis of transmission dynamics reveals synchrony in underlying trans-
49 mission patterns. Integrating these findings into a mathematical model illustrates
50 that the apparent asynchrony can be explained by differences in initial epidemic
51 conditions (i.e., introduction delays and initial susceptibility).

52 **Asynchrony in pertussis epidemics associated with introduc- 53 tion delays**

54 First, to characterize spatial heterogeneity in pertussis waves across Korea, we quan-
55 tify the center of gravity (Figure 1E), which represents the mean timing of cases
56 [1]. Notably, we find a sharp contrast between early (orange) and late (light blue)
57 waves between many neighboring municipalities (Figure 1E), suggesting spatial asyn-
58 chrony in pertussis dynamics. To systematically evaluate this apparent asynchrony,
59 we estimated the spatial synchrony function, which captures changes in correlation

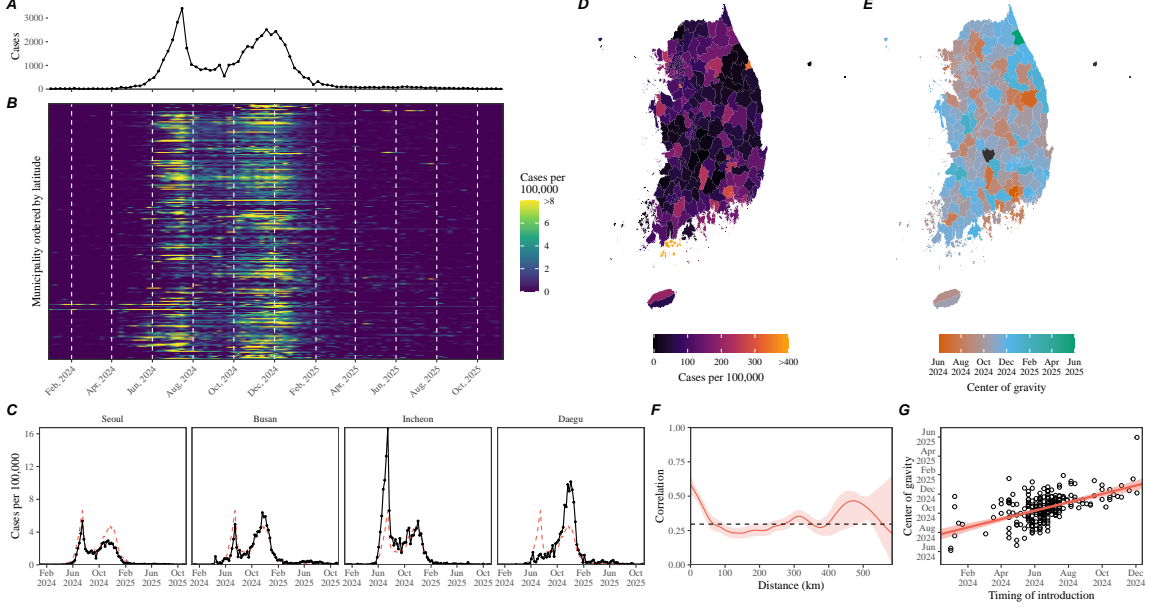


Figure 1: **Spatiotemporal dynamics of pertussis outbreak in Korea, 2024—2025.** (A) Total number of reported cases in Korea. (B) Number of reported cases per 100,000 individuals by municipality, ordered by latitude. (C) Number of reported cases per 100,000 individuals in four most populated cities in Korea. (D) Map of pertussis cases per 100,000 individuals between January 2024 and November 2025. (E) Map of center of gravity, which represents the mean timing of cases. (F) Spatial synchrony in logged cases as a function of distance. The red solid line and shaded regions represent the median estimate and the corresponding 95% confidence interval. The dashed horizontal line represents the mean correlation. (G) Relationship between center of gravity and the timing of introduction, defined as the first week when the number of reported cases is greater than 1 in 100,000. The red solid line and shaded regions represent the linear regression fit and the corresponding 95% confidence interval.

in epidemic dynamics as a function of distance [7]. The spatial synchrony function confirms a sharp reduction in cross-correlation with distance (Figure 1F). For example, within 100km of distance, the cross-correlation drops below 0.25. By comparison, pertussis epidemics in the US maintained cross-correlations above 0.2 even at 1,000 km [14], highlighting the fine-scale asynchrony in pertussis epidemics in Korea. Interestingly, the variation in the center of gravity significantly correlates with the introduction timing ($\rho = 0.53$; 95%CI: 0.44—0.62; Figure 1G), suggesting that differences in introduction timing may contribute to the apparent spatial asynchrony.

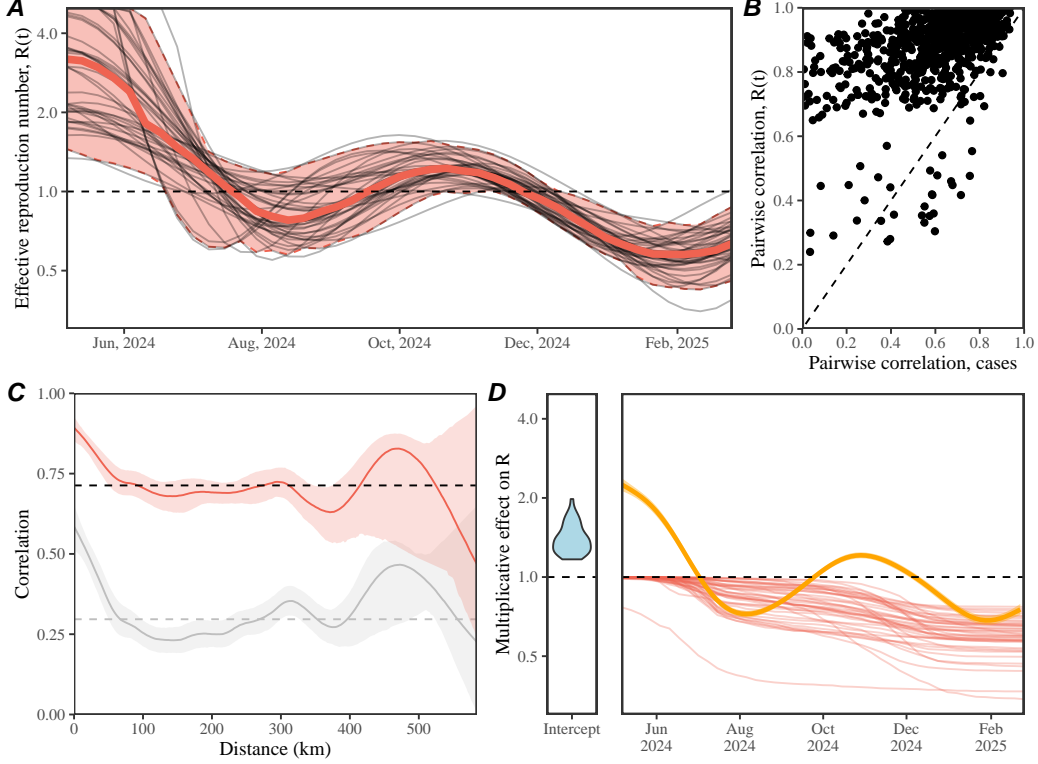


Figure 2: Spatial variation in the estimates of effective reproduction number. (A) Each black line represents the estimated effective reproduction number for a given municipality with more than 400 total cases. The red solid line and shaded regions represent the median and 95% quantiles of effective reproduction number estimates. (B) Relationship between correlation coefficient for $\mathcal{R}(t)$ and correlation coefficient for reported cases across all pairwise municipality combinations with more than 400 total cases. (C) Spatial synchrony in $\mathcal{R}(t)$ (red) versus logged cases (black) as a function of distance. The solid line and shaded regions represent the median estimate and the corresponding 95% confidence interval. The dashed horizontal line represents the mean correlation. (D) Estimated multiplicative effects on $\mathcal{R}(t)$ from the regression analysis. The blue shaded violin represents the distribution of intercept effect, where a separate intercept term is estimated for each municipality. The red lines represent the estimated susceptible depletion effect for each municipality. The orange line and shaded regions represent the estimated changes in transmission from a smooth term and the corresponding 95% confidence interval.

68 Synchrony in temporal changes in pertussis transmission

69 We then ask whether the observed epidemic asynchrony can be explained by the
70 differences in transmission patterns. To do so, we quantify the effective reproduction
71 number $\mathcal{R}(t)$, which measures the average number of new infections caused by a
72 single infected individual [15, 16]. For this analysis, we focus on municipalities with

more than 400 total cases reported because $\mathcal{R}(t)$ estimates can be unstable when the number of infections are low.

Notably, $\mathcal{R}(t)$ estimates appear to be largely homogeneous across different regions, despite the apparent heterogeneity in the observed epidemic dynamics (Figure 2A). Comparisons of correlation coefficients in $\mathcal{R}(t)$ versus correlation coefficients in reported cases between all pairwise municipality combinations confirm this observation (Figure 2B). In 830 out of 861 municipality combinations, correlation in $\mathcal{R}(t)$ is higher than correlation in cases. This is reflected in the spatial synchrony function for $\mathcal{R}(t)$ (Figure 2C), where the mean cross-correlation for $\mathcal{R}(t)$ ($\rho = 0.71$) is considerably higher than that for cases ($\rho = 0.30$).

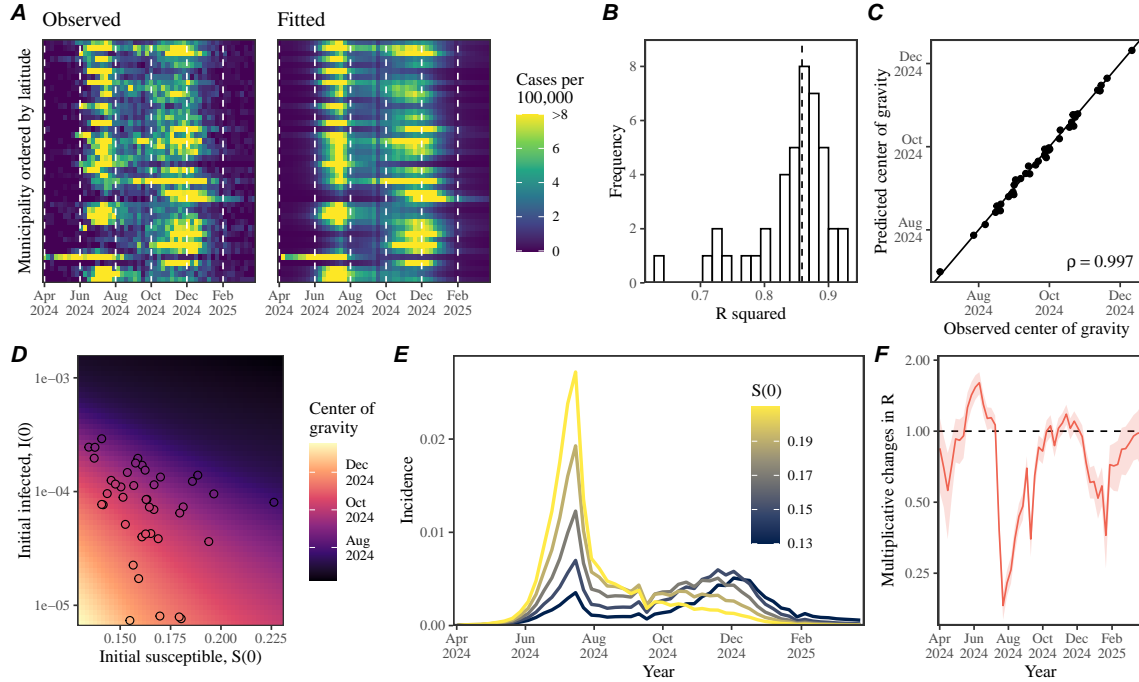


Figure 3: Fine-scale spatiotemporal variation in pertussis epidemic can be explained with a simple SEIR model. (A) Comparisons between the observed and predicted epidemic dynamics across municipalities with more than 400 total cases, ordered by latitude.. (B) The bar plot represents the distribution of R^2 values for model fits. The vertical dashed line represents the median. (C) Relationship between the estimated and predicted center of gravity. The solid line indicated the one-to-one relationship. (D) Relationship between the initial susceptible $S(0)$ and infected $I(0)$ fraction with center of gravity. Points represent the estimates for each municipality. (E) Impact of initial susceptibility on pertussis epidemic dynamics. (F) Estimated time-varying pertussis transmission rate. The red line and shaded regions represent the posterior median and the corresponding 95% credible interval.

To better understand factors driving changes in $\mathcal{R}(t)$, we perform a regression

analysis using a generalized additive model with three covariates [17, 18, 19]: (1) a municipality-level fixed effect allowing each municipality to have its own intercept; (2) a cumulative-cases term capturing the effect of susceptible depletion; and (3) a single smooth term shared across municipalities, which allows for temporal changes in pertussis transmission over time, such as seasonal forcing. First, the smooth term suggests a strong transmission reduction around August and February, which coincide with the timing of school breaks (Figure 2D). Second, the model estimates a significant effect of effect of susceptible depletion (Figure 2D; $p < 0.001$). Notably, this simple regression model explains 84% of variance in $\mathcal{R}(t)$, suggesting that the observed temporal fluctuations in transmission can be largely explained by school-related seasonality and the gradual depletion of susceptible individuals. Taken together, the analysis of center of gravity and $\mathcal{R}(t)$ suggest that differences in introduction timing and susceptible host dynamics are likely main drivers for spatial asynchrony in pertussis epidemics in Korea, rather than variation in seasonal transmission patterns.

Mathematical modeling of fine-scale spatio-temporal pertussis epidemic

To test whether variation in introduction timing and susceptible dynamics alone can explain the observed epidemic patterns, we extended a standard susceptible-exposed-infected-removed (SEIR) model [20] to jointly estimated a single, time-varying transmission term, which is shared across all regions. We also allowed spatial variation in initial susceptible $S(0)$ and infected $I(0)$ fraction as well as the reporting rate ρ . Variation in $S(0)$ captures differences in population-level susceptibility, whereas variation in $I(0)$ effectively captures differences in introduction timing. For this analysis, we also focus on municipalities with more than 400 total cases. The model is fitted using a Bayesian inference software rstan with 4 independent chains, each consisting of 8000 iterations [21]. The convergence was assessed by ensuring low R-hat, high effective sample size, no divergent transitions, and no iterations that exceeded the maximum tree depth.

Our simple transmission model that assume shared transmission rate can capture fine-scale spatiotemporal variation of pertussis outbreak in Korea (Figure 3A) with a median R squared value of 0.86 (95% quantile: 0.71—0.91). Furthermore, we find a near-perfect correlation between the predicted and observed center of gravity (Figure 3C). So what factors determine the timing of epidemic, and therefore the center of gravity? We address this question by simulating our model between April 2024 and April 2025 across plausible ranges of $S(0)$ and $I(0)$.

First, increasing $I(0)$ leads to an earlier epidemic because it permits earlier introduction of the infection to the population (Figure 3D). This is consistent with our earlier observations (Figure 1F). Similarly, increasing $S(0)$ also results in an earlier epidemic. This is because high levels of susceptibility allows for a large first wave, which prevents the second wave through the overcompensatory susceptible depletion

125 (Figure 3E). Finally, we estimate that the large reduction in transmission around
126 late July 2024 and late January 2025 allowed the occurrence of two distinct epidemic
127 waves (Figure 3F). This estimated timing of transmission reduction is consistent with
128 our estimates from the $\mathcal{R}(t)$ analysis and coincide with the timing of school holidays
129 in Korea.

130 We validate our model by taking the estimated transmission term and fitting the
131 remaining parameters (i.e., initial infected, initial susceptible, and reporting proba-
132 bility) to data from the remaining 210 municipalities with less than 400 total cases
133 (Figure S2). While model predictions appear consistent with the observed patterns
134 (Figure S2A), we estimate a lower value for the median R squared: 0.58 (95% quan-
135 tile: 0.04–0.87; Figure S2B). Nonetheless, our analysis suggests that the majority of
136 asynchrony in pertussis epidemics can be explained via the differences in introduction
137 timing and initial susceptibility.

138 Summary

139 Understanding mechanisms that drive spatiotemporal variation in epidemic dynamics
140 is a major aim for infectious disease dynamics and control [1, 2, 3, 4, 7, 8, 9]. The large
141 pertussis outbreaks in Korea that occurred between 2024 and 2025 presents a unique
142 perspective on a fine-scale spatiotemporal asynchrony heterogeneity in epidemic dy-
143 namics: some municipalities experienced two epidemic waves while other places ex-
144 perienced only the first or second without a clear patterns of synchrony. We propose
145 that this variation can be explained by the differences in introduction delays and
146 initial susceptibility, where high levels of susceptibility can cause a large first wave
147 and prevent the second wave through susceptible depletion. Incorporating this idea
148 into a simple transmission model by allowing for a joint estimation of a single trans-
149 mission rate with variation in initial epidemic conditions confirms our hypothesis.
150 Together, these findings demonstrate that differences in initial epidemic conditions—
151 rather than variation in transmission—can generate fine-scale asynchrony, offering
152 a general framework for understanding the spatiotemporal dynamics of re-emerging
153 infections.

154 Caveats and future directions

155 Even though our model explains the observed dynamics reasonably well, there are
156 several limitations to our work. First, our model is purely deterministic and does not
157 account for stochasticity, which is likely an important factor for characterizing the
158 establishment of infections after the initial invasion and the subsequent dynamics,
159 especially in small populations [22, 23, 24]. Second, we estimated that a variation
160 in susceptibility can explain the observed epidemic patterns, but we were unable to
161 identify the mechanism that explains this variation. For example, we hypothesized
162 that past vaccine coverage would explain variation in susceptibility given the role of

163 waning immunity in driving pertussis re-emergence [25, 26, 27], but we did not find
164 a significant correlation (Figure S3).

165 Our parameter estimates must be interpreted with care as our model relies on
166 several simplifying assumptions. For example, we assumed the same values of basic
167 reproduction number \mathcal{R}_0 across all municipalities. Therefore, any regional variation
168 in \mathcal{R}_0 , driven by differences in contact rates and age distributions would be captured
169 in our estimate of the initial susceptible fraction. In other words, our estimated
170 susceptible fraction should be interpreted as the effective susceptibility that also
171 captures behavioral and sociological factors, beyond immunological differences. We
172 also did not consider an age structure in our model, but age-structured contact
173 patterns play an important role in shaping pertussis transmission [20]. For example,
174 [28] recently suggested transmission among elderly may contributed to the persistence
175 of pertussis in Korea. Despite these limitations, our work provides a quantitative
176 foundation and empirical evidence for understanding epidemic asynchrony.

177 Conclusion

178 The continued emergence of new pathogens and re-emergence of vaccine preventable
179 infections, such as pertussis, highlights the importance of identifying hotspots of
180 future outbreaks and developing targeted intervention strategies [29, 30, 31]. The
181 apparent asynchrony in pertussis epidemic in Korea, driven by the differences in in-
182 troduction timing and population-level susceptibility, underlines the importance of
183 detailed pathogen surveillance for early detection and strategic allocation of preven-
184 tion and control resources.. Immunological surveillance platforms will be particularly
185 useful for evaluating potential risk of pathogen re-emergence in the future [32, 33].
186 A detailed understanding of spatial variation in population-level immunity will be
187 crucial for predicting spatiotemporal dynamics of future outbreaks.

188 References

- 189 [1] Virginia E Pitzer, Cécile Viboud, Wladimir J Alonso, Tanya Wilcox, C Jessica
190 Metcalf, Claudia A Steiner, Amber K Haynes, and Bryan T Grenfell. Environmental
191 drivers of the spatiotemporal dynamics of respiratory syncytial virus in
192 the United States. *PLoS pathogens*, 11(1):e1004591, 2015.
- 193 [2] Benjamin D Dalziel, Stephen Kissler, Julia R Gog, Cecile Viboud, Ottar N
194 Bjørnstad, C Jessica E Metcalf, and Bryan T Grenfell. Urbanization and humid-
195 ity shape the intensity of influenza epidemics in US cities. *Science*, 362(6410):75–
196 79, 2018.
- 197 [3] Margarita Pons-Salort, M Steven Oberste, Mark A Pallansch, Glen R Abedi,
198 Saki Takahashi, Bryan T Grenfell, and Nicholas C Grassly. The seasonality of

- 199 nonpolio enteroviruses in the united states: Patterns and drivers. *Proceedings*
200 *of the National Academy of Sciences*, 115(12):3078–3083, 2018.
- 201 [4] Rachel E Baker, Ayesha S Mahmud, Caroline E Wagner, Wenchang Yang, Vir-
202 ginia E Pitzer, Cecile Viboud, Gabriel A Vecchi, C Jessica E Metcalf, and
203 Bryan T Grenfell. Epidemic dynamics of respiratory syncytial virus in current
204 and future climates. *Nature communications*, 10(1):5512, 2019.
- 205 [5] Michael P Hassell, Hugh N Comins, and Robert M Mayt. Spatial structure and
206 chaos in insect population dynamics. *Nature*, 353(6341):255–258, 1991.
- 207 [6] JA Sherratt. Periodic travelling waves in cyclic predator–prey systems. *Ecology*
208 *Letters*, 4(1):30–37, 2001.
- 209 [7] Bryan T Grenfell, Ottar N Bjørnstad, and Jens Kappey. Travelling waves and
210 spatial hierarchies in measles epidemics. *Nature*, 414(6865):716–723, 2001.
- 211 [8] Derek AT Cummings, Rafael A Irizarry, Norden E Huang, Timothy P Endy,
212 Ananda Nisalak, Kumnuan Ungchusak, and Donald S Burke. Travelling waves in
213 the occurrence of dengue haemorrhagic fever in thailand. *Nature*, 427(6972):344–
214 347, 2004.
- 215 [9] Cécile Viboud, Ottar N Bjørnstad, David L Smith, Lone Simonsen, Mark A
216 Miller, and Bryan T Grenfell. Synchrony, waves, and spatial hierarchies in the
217 spread of influenza. *science*, 312(5772):447–451, 2006.
- 218 [10] Robert S Paton, Christopher E Overton, and Thomas Ward. The rapid replace-
219 ment of the SARS-CoV-2 Delta variant by Omicron (B. 1.1. 529) in England.
220 *Science Translational Medicine*, 14(652):eab05395, 2022.
- 221 [11] Hye-Jin Kim, Young Joon Park, Dongkeun Kim, Jihee Lee, Yun Kyoung
222 Kim, Soonryu Seo, Jin Seon Yang, Yeojeun Yun, Eunbyeol Wang, Subin Park,
223 Seo Yeon Ko, Jin Lee, Jeeyeon Shin, Woocheon Lee, and Seonhee Ahn. Pertussis
224 surveillance and occurrence report in the Republic of Korea: from 2024 to the
225 first half of 2025. *Public Health Weekly Report*, 18(43):1631–1651, 11 2025.
- 226 [12] Hyun Mi Kang, Taek-Jin Lee, Su Eun Park, and Soo-Han Choi. Pertussis in
227 the post-COVID-19 era: resurgence, diagnosis, and management. *Infection &*
228 *Chemotherapy*, 57(1):13, 2024.
- 229 [13] Scott M Duke-Sylvester, Luca Bolzoni, and Leslie A Real. Strong seasonality
230 produces spatial asynchrony in the outbreak of infectious diseases. *Journal of*
231 *the Royal Society Interface*, 8(59):817–825, 2011.
- 232 [14] Marc Choisy and Pejman Rohani. Changing spatial epidemiology of pertussis
233 in continental USA. *Proceedings of the Royal Society B: Biological Sciences*,
234 279(1747):4574–4581, 2012.

- 235 [15] Jacco Wallinga and Marc Lipsitch. How generation intervals shape the relationship
236 between growth rates and reproductive numbers. *Proceedings of the Royal Society B: Biological Sciences*, 274(1609):599–604, 2007.
- 238 [16] Anne Cori, Neil M Ferguson, Christophe Fraser, and Simon Cauchemez. A new framework and software to estimate time-varying reproduction numbers during
239 epidemics. *American journal of epidemiology*, 178(9):1505–1512, 2013.
- 241 [17] Dennis E te Beest, Michiel van Boven, Mariëtte Hooiveld, Carline van den Dool,
242 and Jacco Wallinga. Driving factors of influenza transmission in the netherlands.
243 *American journal of epidemiology*, 178(9):1469–1477, 2013.
- 244 [18] Simon N Wood. *Generalized additive models: an introduction with R*. Chapman
245 and Hall/CRC, 2017.
- 246 [19] Stephen M Kissler, Christine Tedijanto, Edward Goldstein, Yonatan H Grad,
247 and Marc Lipsitch. Projecting the transmission dynamics of SARS-CoV-2 through the postpandemic period. *Science*, 368(6493):860–868, 2020.
- 249 [20] Pejman Rohani, Xue Zhong, and Aaron A King. Contact network structure
250 explains the changing epidemiology of pertussis. *Science*, 330(6006):982–985,
251 2010.
- 252 [21] Bob Carpenter, Andrew Gelman, Matthew D Hoffman, Daniel Lee, Ben
253 Goodrich, Michael Betancourt, Marcus Brubaker, Jiqiang Guo, Peter Li, and
254 Allen Riddell. Stan: A probabilistic programming language. *Journal of statistical software*, 76:1–32, 2017.
- 256 [22] Bärbel F Finkenstädt, Ottar N Bjørnstad, and Bryan T Grenfell. A stochastic
257 model for extinction and recurrence of epidemics: estimation and inference for
258 measles outbreaks. *Biostatistics*, 3(4):493–510, 2002.
- 259 [23] James O Lloyd-Smith, Sebastian J Schreiber, P Ekkehard Kopp, and Wayne M
260 Getz. Superspreading and the effect of individual variation on disease emergence.
261 *Nature*, 438(7066):355–359, 2005.
- 262 [24] FMG Magpantay, M Domenech De Cellés, P Rohani, and AA King. Pertussis
263 immunity and epidemiology: mode and duration of vaccine-induced immunity.
264 *Parasitology*, 143(7):835–849, 2016.
- 265 [25] Helen J Wearing and Pejman Rohani. Estimating the duration of pertussis
266 immunity using epidemiological signatures. *PLoS pathogens*, 5(10):e1000647,
267 2009.
- 268 [26] Tina Tan, Tine Dalby, Kevin Forsyth, Scott A Halperin, Ulrich Heininger,
269 Daniela Hozbor, Stanley Plotkin, Rolando Ulloa-Gutierrez, and Carl
270 Heinz Wirsing Von König. Pertussis across the globe: recent epidemiologic

- 271 trends from 2000 to 2013. *The Pediatric infectious disease journal*, 34(9):e222–
272 e232, 2015.
- 273 [27] Matthieu Domenech de Cellès, Felicia MG Magpantay, Aaron A King, and Pej-
274 man Rohani. The impact of past vaccination coverage and immunity on pertussis
275 resurgence. *Science translational medicine*, 10(434):eaaj1748, 2018.
- 276 [28] Seonghui Cho, Dong Wook Kim, Chiara Achangwa, Junseo Oh, and Sukhyun
277 Ryu. Pertussis in the elderly: Plausible amplifiers of persistent community
278 transmission of pertussis in South Korea. *Journal of Infection*, 89(3), 2024.
- 279 [29] David L Heymann and Guénaël R Rodier. Hot spots in a wired world: Who
280 surveillance of emerging and re-emerging infectious diseases. *The Lancet infec-*
281 *tious diseases*, 1(5):345–353, 2001.
- 282 [30] Mahmoud M Naguib, Patrik Ellström, Josef D Järhult, Åke Lundkvist, and
283 Björn Olsen. Towards pandemic preparedness beyond COVID-19. *The Lancet*
284 *Microbe*, 1(5):e185–e186, 2020.
- 285 [31] Hai Nguyen-Tran, Sang Woo Park, Kevin Messacar, Samuel R Dominguez,
286 Matthew R Vogt, Sallie Permar, Perdita Permaul, Michelle Hernandez, Daniel C
287 Douek, Adrian B McDermott, et al. Enterovirus D68: a test case for the use of
288 immunological surveillance to develop tools to mitigate the pandemic potential
289 of emerging pathogens. *The Lancet Microbe*, 3(2):e83–e85, 2022.
- 290 [32] Michael J Mina, C Jessica E Metcalf, Adrian B McDermott, Daniel C Douek,
291 Jeremy Farrar, and Bryan T Grenfell. A global immunological observatory to
292 meet a time of pandemics. *Elife*, 9:e58989, 2020.
- 293 [33] Hai Nguyen-Tran, Sang Woo Park, Matthew R Vogt, Perdita Permaul, Alicen B
294 Spaulding, Michelle L Hernandez, Jennifer A Bohl, Sucheta Godbole, Tracy J
295 Ruckwardt, Peter W Krug, et al. Dynamics of endemic virus re-emergence in
296 children in the USA following the COVID-19 pandemic (2022–23): A prospec-
297 tive, multicentre, longitudinal, immunoepidemiological surveillance study. *The*
298 *Lancet Infectious Diseases*.